# Crupi2013jpcbBis

**DATASET** · OCTOBER 2013

READS
46

**8 AUTHORS**, INCLUDING:

Vincenza Crupi
Università degli Studi di Messina
**162** PUBLICATIONS **1,624** CITATIONS
SEE PROFILE

Graziano Guella
Università degli Studi di Trento
**240** PUBLICATIONS **3,117** CITATIONS
SEE PROFILE

Valentina Venuti
Università degli Studi di Messina
**137** PUBLICATIONS **1,446** CITATIONS
SEE PROFILE

THE JOURNAL OF PHYSICAL CHEMISTRY B

Article

pubs.acs.org/JPCB

# Influence of Chirality on Vibrational and Relaxational Properties of (*S*)- and (*R*,*S*)-Ibuprofen/methyl-β-cyclodextrin Inclusion Complexes: An INS and QENS Study

Vincenza Crupi,[†] Graziano Guella,[‡] Stéphane Longeville,[§] Domenico Majolino,*[,†] Ines Mancini,[‡] Alessandro Paciaroni,[∥] Barbara Rossi,[‡,⊥] and Valentina Venuti[†]

[†]Dipartimento di Fisica e di Scienze della Terra, Università di Messina and CNISM UdR Messina, Viale Ferdinando Stagno D'Alcontres 31, 98166 Messina, Italy

[‡]Dipartimento di Fisica, Università di Trento, via Sommarive 14, 38123 Povo, Trento, Italy

[§]Laboratoire Léon Brillouin (CEA/CNRS), CEA Saclay, 91191 Gif-sur-Yvette Cedex, France

[∥]Dipartimento di Fisica, Università di Perugia and CNR-INFM CRS SOFT, Via A. Pascoli, 06123 Perugia, Italy

[⊥]Dipartimento di Informatica, Università di Verona, Strada le Grazie 15, 37134 Verona, Italy

**ABSTRACT:** In this paper, we analyze the internal picosecond dynamics of enantiomeric ((*S*)-) and racemic ((*R*,*S*)-) ibuprofen (IBP), when forming inclusion complexes, in solid state, with methyl-β-cyclodextrin (Me-β-CD), by inelastic and quasi elastic neutron scattering. The study was aimed at understanding, by the analysis of the vibrational and relaxational properties of the inclusion complexes also with respect to the single components, if and how the differences in the structural properties of the hydrogen bond (HB) network of (*S*)- and (*R*,*S*)-IBP can have influence on the complexation process triggered by "host−guest" interactions, whose detailed knowledge is retained as a prerequisite for enantiodiscrimination. From the results, a similar complexation mechanism for (*S*)- and (*R*,*S*)-IBP is argued, with a preferred penetration mode involving the isopropyl group of IBP.

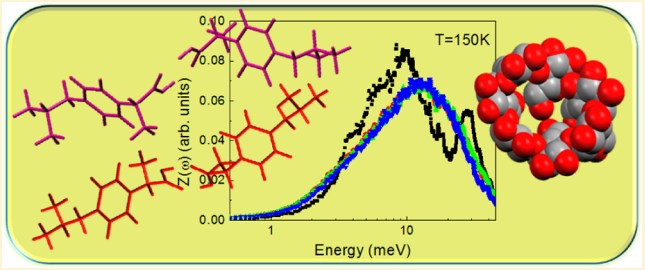


## INTRODUCTION

Chiral discrimination represents one of the most interesting subjects in chemistry, being at the basis of a number of processes, such as asymmetric synthesis, enzymatic catalysis, and techniques as gas and liquid chromatography and capillary electrophoresis.[1] Enantiorecognition assumes a fundamental role especially in the development, use, and action of pharmaceutical agent, due to the different physiological and toxicological properties of each antipode.[2]

Cyclodextrins (CDs) are cyclic oligosaccharides formed by six (α-CD), seven (β-CD), or eight (γ-CD) α-(1 → 4) linked chiral glucopyranose units, resulting in a toroidal structure.[3] As is well-known, they have the capability of including a wide range of appropriate guest molecules into their hydrophobic cavities via noncovalent and hydrophobic interactions, i.e., entropic effect.[4−6] Again, due to their asymmetric centers, CDs have the ability to discriminate between suitable enantiomers, forming diastereomeric complexes with slightly different stabilities.[7−9]

For this reason, great effort has been paid over the past few years in the experimental and theoretical investigation of chiral and molecular recognition by selective complexation of thousands of enantiomers in CDs and their derivatives.[10−12] Studies in aqueous phase allowed the determination of the binding constants[13] and of the thermodynamic parameters,[14] whereas, in solid state, information on the mechanism of chiral recognition has been attempted by the geometrical features as probed by X-ray diffraction.[9] Besides experimental measurements, computer simulation methods, i.e., molecular mechanics and molecular dynamics methods, have been largely employed to accurately estimate, according to a variety of proposed models, the free energy of binding ($\Delta G_{binding}$) and the structure.[10,15] The results indicated, as main factors contributing to the enantiodifferentiation, the tight fit of the guest into the cavity, solvent interactions, the hydrogen bonding potential of the guest, and the crystal packing arrangement of the host.[16] In spite of this, the basic principles of the enantioselective recognition are not fully understood at atomic level, and there is no model available that can describe in a universal way the complexation mechanism in CDs as well as the chiral separation.[17]

Ibuprofen (IBP, 4-isobutyl-2-phenylpropionic acid), one of the most effective and widely used nonsteroidal analgesics and anti-inflammatory agents,[18,19] contains in its chemical structure a stereogenic carbon, and thus it can exist in two enantiomeric forms, (*R*)- and (*S*)-ibuprofen (see Figure 1).

**Received:** March 29, 2013
**Revised:** September 6, 2013
**Published:** September 9, 2013





dx.doi.org/10.1021/jp403099a | *J. Phys. Chem. B* 2013, 117, 11466−11472

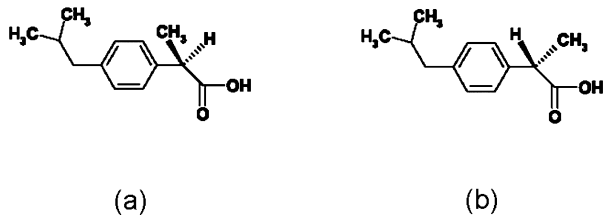


**Figure 1.** Structure of the two enantiomers of IBP: (a) (*R*)-IBP, (b) (*S*)-IBP. Notation: full wedge, bond outgoing; empty wedge, bond ingoing.

(*R*)- and (*S*)-IBP exhibit different pharmacological performances; in particular, only (*S*)-IBP is biologically active and primarily responsible for the anti-inflammatory activity of the drug. Nevertheless, IBP is currently clinically used as the racemate (*R,S*)-IBP form, because in vivo the (*R*)-form is continuously metabolically converted into the (*S*)-form.[20] The differences in the properties of the chiral and racemic IBP states should be sought in the intramolecular dynamics and structure and in the properties of the hydrogen bond (HB) networks.[21,22] Structural studies[23,24] on IBP enantiomers and racemate revealed that in crystal lattices of both (*S*)- and (*R,S*)-IBP molecules are arranged to form a cyclic dimer through hydrogen bonds between their carboxylic groups, COOH. Thermodynamics of sublimation, crystal lattice energies, and crystal structures of (*R,S*)-, (*S*)-, and (*R*)-IBP have also been characterized[21,22] in order to understand the differences of drug−drug intermolecular interactions in the two cases. This information is the basic knowledge needed for a rational development of the appropriate method for the resolution of racemate. In liquid phase, experimental studies, corroborated by atomistic molecular mechanics simulations, concerning chiral discrimination of IBP isomers revealed an energetically and conformationally preferred penetration mode in *β*-CD involving the (*S*)-IBP isomer.[25] Again, in aqueous solution, (*S*)-IBP has been proven to form more stable inclusion complexes with hydroxypropyl-*β*-cyclodextrin (HP-*β*-CD) as compared with (*R,S*)-IBP.[26] On the contrary, relatively few studies have been reported in solid phase.

Recently, we reported on the modifications produced by inclusion, in solid state, into native *β*-CD and synthetically modified methyl-*β*-CD (Me-*β*-CD) (see Figure 2) on the vibrational spectra of (*R,S*)-IBP, by using Fourier transform infrared spectroscopy in the attenuated total reflectance geometry (FTIR-ATR) and density functional theory (DFT) calculations.[27]

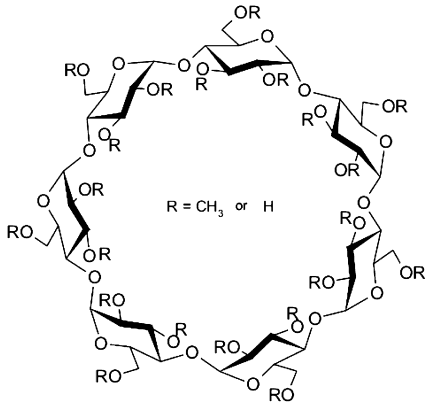


**Figure 2.** Molecular structure of methyl-*β*-cyclodextrin (Me-*β*-CD).

From temperature-dependent studies, the enthalpy changes associated with "host−guest" interactions in the solid phase have been estimated and the obtained results reveal Me-*β*-CD to be the optimal partner for IBP. Then, a quantitative analysis on the influence of chirality of IBP on the complexation mechanism, i.e., geometry and/or thermal stability of inclusion complexes, has been performed by investigating the modifications induced in vibrational FTIR-ATR spectra, in the C=O stretching region, of complexes formed by Me-*β*-CD with the two pure enantiomeric and the racemic forms of IBP.[28] A higher stability has been revealed in the case of the complexes formed by the enantiomers with respect to racemate, ascribed to the increased difficulty, in this latter case, in breaking the intermolecular dimeric hydrogen bond between (*R*)- and (*S*)-IBP molecules in the racemic form, proven to constitute the first step for complexation. Here, we went deeper inside the low-frequency vibrational and relaxational dynamics on solid (*S*)-IBP/Me-*β*-CD and (*R,S*)-IBP/Me-*β*-CD inclusion complexes, compared to that of the single components, carrying out an incoherent neutron scattering investigation, in order to clarify the complexation process, and trying to understand if and how dynamical properties, in the ps−ns time scale, of the hydrogen bond (HB) network of enantiomer with respect to racemate can affect the complexation mechanism.

## EXPERIMENTAL METHODS

**A. Synthesis of CD Complexes.** Methyl-*β*-cyclodextrin (Me-*β*-CD, degree of substitution ∼1.6−2.0) was purchased from Fluka Chemie (Switzerland). (*R,S*)- and (*S*)-IBP were acquired from Sigma-Aldrich. All reagents were used without further purification. For the synthesis of complexes, Me-*β*-CD (65.5 mg, 0.05 mmol) was dissolved in water (0.5 mL) to obtain a 0.1 mM solution; subsequently, another 1 mL of water was added and the mixture was stirred at 50 °C in order to obtain a solution. An equimolar amount of dry (*R,S*)- or (*S*)-IBP (10.4 mg, 0.05 mmol) was added to this solution and the resulting dispersion was stirred at 50 °C for 2 h to obtain a white dispersion. The liquid phase was removed and both the evaporated supernatant and the precipitate were dried in a vacuum chamber, using $P_2O_5$ as dehydratant. Electrospray ionization mass spectrometry (ESI-MS, Bruker Esquire spectrometer) measurements and nuclear magnetic resonance (NMR, Bruker Avance 400 spectrometer) analysis allowed verification of the effective complex formation and to obtain information on its stoichiometry, which turned out to be 1:1.[29]

**B. Neutron Scattering Experiments.** Neutron scattering experiments were performed at Laboratoire Léon Brillouin (LLB, Saclay, France) using the time-of-flight (TOF) spectrometer MIBEMOL. Measurements were carried out at $T$ = 150 K and $T$ = 300 K using neutrons with an incident wavelength of 6 Å, with an exchanged wavevector $Q$-independent experimental resolution of 90 $\mu$eV (defined as the full-width half-maximum of a vanadium standard). The covered $Q$-range was from 0.49 $Å^{-1}$ to 1.73 $Å^{-1}$. The recorded spectra have been binned into 10 groups to improve the counting statistics. The explored energy range was from −45 meV to about 1.4 meV. In all of the figures of this paper the sign of the energy transfer has been changed for sake of simplicity. As sample holder, a standard, indium sealed, flat aluminum cell, with variable internal spacing was used. In particular, a thickness of 0.2 mm was used for (*S*)- and (*R,S*)-


dx.doi.org/10.1021/jp403099a | J. Phys. Chem. B 2013, 117, 11466−11472

IBP, and for their inclusion complexes with Me-$\beta$-CD, whereas a thickness of 0.5 mm was used for Me-$\beta$-CD. For each measurement, the sample holder was placed at an angle of 135° with respect to the incident beam direction. The time of data acquisition was about 12 h. A transmission of ∼96% was obtained for IBP, of ∼91% for Me-$\beta$-CD, of ∼94% for IBP/Me-$\beta$-CD inclusion complexes. An estimate of the multiple scattering using the simplified Sears formula[30] confirms that it is below 10% on the elastic peak for all systems, thus affecting in a similar way all the analyzed samples, so multiple scattering contributions have been neglected. We expect that, in the end, the values of the parameters estimated from the fit of the quasielastic part of the spectra (see below) would not be affected too much even taking into account the multiple scattering contribution; as such, a contribution is a small fractional contribution of total scattering with a smooth $Q$-dependence. Also, in the inelastic region both multiple scattering and multiphonon scattering are expected to give a significant contribution, thus changing the amplitude of the calculated vibrational density of states. However, a thorough estimate of these components is usually not an easy task, as a detailed model for the system is required. Multiple scattering depends on the true dynamic structure factor; in particular, the elastic−quasielastic/inelastic events give rise to the main contribution to multiple scattering.[30] In the incoherent approximation, the elastic−quasielastic contribution depends principally on the total cross section, that is practically the same in the present samples, despite the fact that they have different chemical composition. Multiphonon contribution as well may significantly contribute to the density of states in the high energy region; however, we expect this contribution to be rather smooth and not producing additional peaks. Thus, since we are interested in a relative comparison among samples with very similar total cross sections, the relevant features should be quite similar to the curve calculated without inclusion of multiple scattering and multiphonon components.

The measured time-of-flight spectra were analyzed with QENSH data treatment program, available at LLB, that allows calibration of the detectors with the vanadium spectra, correction for the empty cell, transformation of the TOF spectra into energy spectra, data grouping to improve signal/noise ratio, and finally the data fitting of the quasi elastic broadening by a proper scattering law.[31]

For the systems under investigation, the dominant contribution to the revealed signal is the large number of hydrogen atoms, characterized by a very large, almost exclusively incoherent, neutron cross section ($\sigma_{inc} \sim 79.90$ barns, $\sigma_{coh} \sim 1.76$ barns), by far higher than the coherent or incoherent cross section of any other element.[31] Therefore, the neutron scattered intensity will be related to the so-called incoherent dynamic structure factor (or incoherent scattering function) $S_{inc}(Q,\omega)$.[32−36] In the one-phonon approximation, $S_{inc}(Q,\omega)$ can be written, at a given temperature $T$, as[32]

$$S_{inc}(Q,\omega) = e^{-2W(Q,T)}\{A_0(Q)\delta(\omega) + [1 - A_0(Q)]S_{QE}(Q,\omega) + S_{INEL}(Q,\omega)\} \otimes R(Q,\omega) \quad (1)$$

$S_{inc}(Q,\omega)$ is splitted into the sum of three components. The first term $A_0(Q)\delta(\omega)$ represents the elastic response of the system, due to those scattering events which do not involve change in energy, whose $\omega$-dependence is accounted for by a Dirac delta function, $\delta(\omega)$. The $Q$-dependence is provided by the factor $A_0(Q)$, which in fact represents the space-Fourier transform of the scatterers' distribution, taken at infinite time and averaged over all the possible initial positions. The second term $[1 - A_0(Q)]S_{QE}(Q,\omega)$ is the quasielastic scattering contribution, which appears in the experimental spectra as a broadening of the elastic peak and gives information about the diffusive and relaxational movements. Since in the incoherent approximation the integral over the whole energy range of the dynamic structure factor is $Q$-independent, eq 1 implies that $A_0(Q)$ can be directly estimated as the fraction of the total neutron scattering contributing to the elastic peak.

Due to the complexity of the structure of the systems under investigation, many different kinds of motions can give rise to quasielastic scattering. On one side, the movements of the highly diversified molecular subunits produce quite different quasielastic contributions. On the other side, even identical subunits may experience different local environments and thus move in different ways. It is therefore very difficult to find an exact theoretical function to describe the quasielastic scattering term.

It is then more useful to model $S_{QE}(Q,\omega)$ through a phenomenological function, described as a sum of Lorentzians:[37,38]

$$[1 - A_0(Q)]S_{QE}(Q,\omega) = \sum_n QISF_n(Q)L_n(\sigma_n,\omega) \quad (2)$$

where $L_n(\sigma_n,\omega)$ is the $n$th Lorentzian, $\sigma_n$ is its full width at half-maximum (fwhm), the inverse of which provides an estimate of the characteristic time scale of the corresponding motion, and $QISF_n(Q)$ is the quasielastic incoherent structure factor, which provides the energy integral of the $n$th quasielastic component and quantifies the degree of activity of the relevant motion. As a matter of fact, the dynamical heterogeneity of the hydrogen atoms in the system gives origin to a variety of quasielastic components in the spectra, and every Lorentzian represents, rather than a single kind of movement, a broad, almost continuous distribution of motions, each characterized by its own correlation time and related line width. Thus, in this context, $\sigma_n$ should be regarded as an "effective" line width, whereas $QISF_n(Q)$ should be considered a quantitative measure of the activated dynamical processes which $L_n$ represents.

The third term, $S_{INEL}(Q,\omega)$, is the inelastic incoherent scattering function. Due to the low energy of incident neutrons of the present experiment, the inelastic neutron scattering (INS) spectrum is mainly an energy-gain spectrum, because neutrons gain energy by excited vibrational modes. Since nuclear interactions are not subject to dipole or polarizability selection rules, INS is sensitive to modes at all wavevectors across the Brillouin zone.

From $S_{INEL}(Q,\omega)$ we directly estimated the one-phonon vibrational density of states (VDOS) $Z(\omega)$ through the relation[39]

$$Z(\omega) = \frac{2M\omega S_{INEL}(Q,\omega)}{Q^2\{1 + n(\omega,T)\}\exp\{-2W(Q,T)\}} \quad (3)$$

where $n(\omega,T)$ is the Bose-Einstein factor defined by $\{\exp(\hbar\omega/k_BT) - 1\}^{-1}$, and $2W(Q,T) = Q^2\langle u^2(T)\rangle$, is the Debye−Waller factor (DWF), that also appears in front of eq 1. It describes the Gaussian $Q$-decreasing due to the vibrational atomic mean square displacement $\langle u^2(T)\rangle$. In particular, eq 3 has been integrated over the entire angular range to calculate the VDOS for all the measured samples.[40] In calculating the VDOS, no correction for multiphonon processes was attempted, as the

contributions are small at the temperatures and $Q$-values covered by the present experiment. The VDOS have been normalized to their integral up to 20 meV, i.e., in the first part of the phonon translational region.

Finally we notice that $R(Q,\omega)$ is the instrumental energy resolution function, which has a finite characteristic line width. The inverse of such line width determines the time scale of the slowest observable motion.

## RESULTS AND DISCUSSION

**A. INS Analysis.** In Figure 3 we display the dynamical structure factor of (*S*)-IBP, (*R*,*S*)-IBP, and Me-$\beta$-CD at $T$ = 150 K. Only a broad peak at ∼2 meV can be observed for Me-$\beta$-CD. This feature, which is reminiscent of the so-called Boson peak usually found in the spectra of glassy materials,[41] suggests that the cyclodextrin has a prevalent amorphous character. As we will see below in Figure 5, a behavior quite similar to that is also shown by the complexes under investigation. On the other hand, the peaks at ∼4 meV and ∼7.5 meV in the (*R*,*S*)-IBP spectrum seem to correspond to motions associated to the intermolecular and collective vibrations in the crystalline state already observed by Raman scattering.[42] By analogy, also, the peak at ∼4 meV and the shoulders at ∼5 and ∼10 meV in the (*S*)-IBP spectrum would correspond to phonon bands typical of the crystalline phase. This behavior suggests that both the (*R*,*S*)-IBP and the (*S*)-IBP systems consist of prevalent crystalline phases. Quite interestingly, the low-frequency inelastic features of these two systems are quite distinct, thus indicating that their different geometrical arrangement reflects as well into peculiar large amplitude vibrational motions.

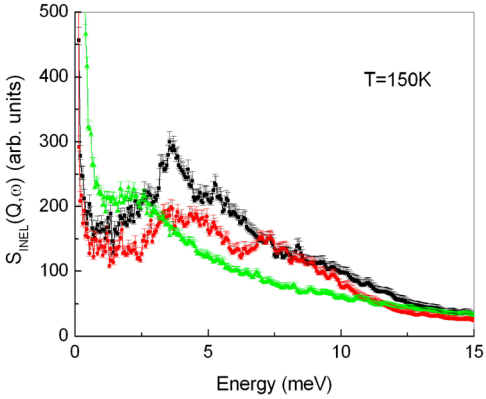


**Figure 3.** Experimental inelastic incoherent scattering function $S_{INEL}(Q,\omega)$ of (*S*)-IBP (black squares), (*R*,*S*)-IBP (red circles), and Me-$\beta$-CD (green up triangles) at $T$ = 150 K.

The vibrational density of states (VDOS) $Z(\omega)$ calculated by using eq 3 is reported in Figure 4 for (*S*)-IBP and (*R*,*S*)-IBP at $T$ = 150 K. As the VDOS have been normalized with respect to their integral, they represent in the incoherent approximation the average vibrational behavior of the hydrogen atoms belonging to the system under investigation.

From a general inspection of the figure, it seems that the low-energy behavior of both systems up to ∼3 meV is well reproduced by a quadratic trend, i.e., that of a Debye-like continuous elastic model ($\sim\omega^2$), thus supporting the crystalline state of the systems. In addition, a shoulder at about 5 meV and a peak at about 9−10 meV, which represent the contributions of phonon branches already observed in Figure 3, are even more visible for both systems. Also in this representation, the vibrational features of the enantiomer and the racemate are quite distinct, in particular in the region around 10 meV, where the peak is larger in the (*R*,*S*)-IBP sample with respect to (*S*)-IBP. The peak at ∼27 meV, well evident in both (*S*)-IBP and (*R*,*S*)-IBP spectra, is ascribed to the torsional modes (rotational oscillations) of methyl ($CH_3$) groups.

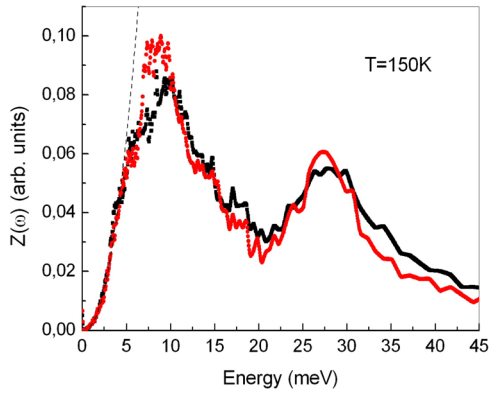


**Figure 4.** Experimental vibrational density of states $Z(\omega)$ of (*S*)-IBP (black squares), (*R*,*S*)-IBP (red circles), at $T$ = 150 K. Dashed lines represent the Debye-like continuous elastic model ($\sim\omega^2$). The error bars range between ∼1% and ∼10% for the highest energies, they have not been shown for sake of clarity.

Figure 5 reports the vibrational density of states $Z(\omega)$ of (*S*)-IBP/Me-$\beta$-CD and (*R*,*S*)-IBP/Me-$\beta$-CD inclusion complexes, and of Me-$\beta$-CD, always at $T$ = 150 K.

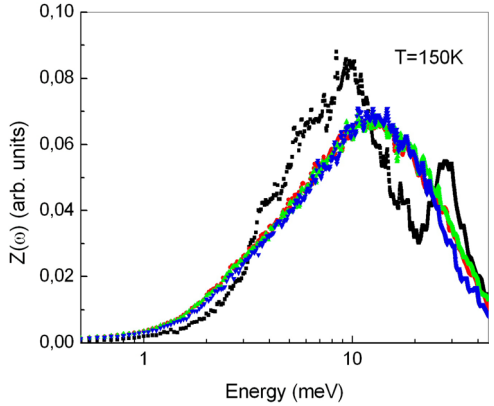


**Figure 5.** Log-lin plot of the experimental vibrational density of states $Z(\omega)$ of (*S*)-IBP/Me-$\beta$-CD inclusion complex (red circles), (*R*,*S*)-IBP/Me-$\beta$-CD inclusion complex (green up triangles), and Me-$\beta$-CD (blue down triangles) at $T$ = 150 K. For comparison, the experimental density of vibrational states $Z(\omega)$ of (*S*)-IBP is also reported (black squares). The error bars range between ∼1% and ∼10% for the highest energies; they have not been shown for the sake of clarity.

As immediately appears evident, after the inclusion inside the CD cavity, the vibrational behavior of enantiomer and racemate is almost the same, and tends to reproduce the shape of the cyclodextrin itself. This suggests, on one hand, a similar complexation mechanism for (*S*)-IBP and (*R*,*S*)-IBP, according to what was already revealed by previous FTIR-ATR measurements.[28] Quite interestingly, in the low-frequency region up to ∼3 meV, the VDOS of these systems shows an excess of vibrational states with respect to that of the (*S*)-IBP sample, i.e., a boson peak, thus confirming their glass-like behavior. In addition, no clear peak at ∼27 meV for $CH_3$ librational motions


dx.doi.org/10.1021/jp403099a | J. Phys. Chem. B 2013, 117, 11466−11472

can be detected in the VDOS of (*S*)-IBP/Me-*β*-CD and (*R*,*S*)-IBP/Me-*β*-CD inclusion complexes, even though in the region from 20 to 40 meV their VDOS are definitely higher than that of pure Me-*β*-CD. This small extra-component can be attributed to the IBP's $CH_3$ librational motions, which appear less intense as the IBP incoherent signal is much less strong than that of Me-*β*-CD component as the molar fraction IBP:Me-*β*-CD of 1:1 corresponds to a relative weight of 1:10. On the other hand, since no $CH_3$ librational peak is detectable in the VDOS of the Me-*β*-CD component, we conclude that methyl groups belonging to this system only undergo free, possibly slow rotations, as they are not even visible as a quasielastic broadening.

In particular, the observed appearance, in the VDOS of (*S*)-IBP/Me-*β*-CD and (*R*,*S*)-IBP/Me-*β*-CD inclusion complexes, of an excess of intensity at around 30 meV, is indicative of a hindering of the $CH_3$ rotational motion upon complexation, because of the restriction of this functional group into the hydrophobic cavity of Me-*β*-CD. This is compatible with a favored complexation geometry in which the isopropyl group of ibuprofen is wrapped inside the cyclodextrin cavity, confirming what was already hypothesized by molecular dynamics simulation and Raman and FTIR-ATR measurements.[27−29]

**B. QENS Analysis.** As previously mentioned, we fitted our experimental QENS spectra as a sum of Lorentzians convoluted with the instrumental resolution function. In particular, the spectra have been adequately reproduced by using only one Lorentzian component, $L(\sigma,\omega)$, with line width $\sigma$, describing the sub-meV broadening of the elastic peak and a flat background. The addition of further components did not significantly improve the fit quality. The quasielastic signal has been fitted in the energy range from −1 to 0.2 meV.

No quasi-elastic contribution has been revealed for all the investigated systems at $T$ = 150 K. This was in a way expected, since this temperature is below the dynamical transition temperature ($T_d \cong$ 220−230 K) already revealed, by previous elastic incoherent neutron scattering (EINS) measurements, in *β*-cyclodextrin and its inclusion complexes with guest molecules similar to ibuprofen.[43] On the contrary, at $T$ = 300 K the quasi-elastic signal can be immediately noted in the spectra of Me-*β*-CD, as well as in the inclusion complexes, revealing an anharmonic internal dynamics that can be related to the relaxation of the hydrogen bonding network formed by the hydroxyl groups (OH groups of IBP, primary and secondary OH groups of Me-*β*-CD) and crystallization residual water molecules.[34] Again, in the case of inclusion complexes, the well-known amorphization associated with complexation[44−49] will also contribute to the activation of additional degrees of freedom over the harmonic behavior. On the contrary, a purely elastic peak has been revealed at this temperature for pure racemic and enantiomeric IBP. This is reasonable, as these systems do not contain plasticizing water molecules, and are hence supposed to behave mainly like a harmonic solid, in a semicrystalline phase, at least in the explored T-range. Also, possible rotational motions of $CH_3$ groups of IBP are likely too slow to be resolved with the current energy resolution, as happens in polymeric systems.[50]

Then, the fit of $S_{QE}(Q,\omega)$ has been performed, according to eq 2, only for the inclusion complexes (*S*)-IBP/Me-*β*-CD and (*R*,*S*)-IBP/Me-*β*-CD, and for the Me-*β*-CD, at $T$ = 300 K.

In Figure 6 we report, as an example, the semilog plot of the experimental QENS spectra for (*S*)-IBP/Me-*β*-CD (a) and (*R*,*S*)-IBP/Me-*β*-CD (b) inclusion complexes, at $Q$ = 1.59 Å$^{-1}$, along with the combined fitting functions.

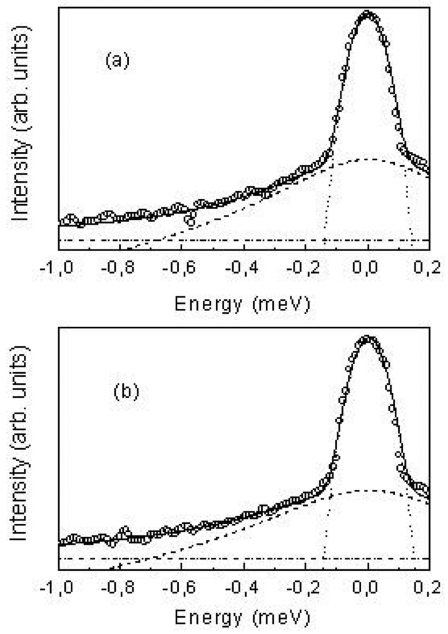


**Figure 6.** Semi-log plot of the quasi elastic neutron scattering spectra of (*S*)-IBP/Me-*β*-CD (a) and (*R*,*S*)-IBP/Me-*β*-CD (b) inclusion complexes, at $Q$ = 1.59 Å$^{-1}$. Open circles: experimental data points; the experimental error bars are smaller than the plotted data points. Full line: best fit function. Dashed line: Lorentzian component. Dotted line: elastic peak. Dash-dotted line: linear background.

Inside the volume explored by the moving protons, the dynamics is described by the $Q$-variations of the line width $\sigma$ of the Lorentzian quasi-elastic contribution. This line width is reported in Figure 7 over the whole explored $Q$-range, for (*S*)-IBP/Me-*β*-CD and (*R*,*S*)-IBP/Me-*β*-CD inclusion complexes, and for the Me-*β*-CD.

The independence of the half-width of $L(Q,\omega)$ versus $Q$ is a signature of a confined dynamics. The characteristic times of the corresponding motions are quite similar for all the samples, resulting to be $\tau$ = 2.4 ± 0.1 ps for the (*R*,*S*)-IBP/Me-*β*-CD

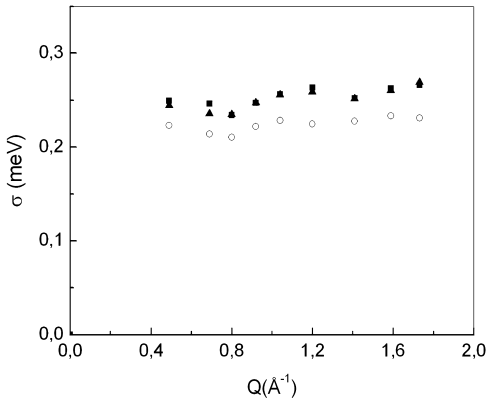


**Figure 7.** Linewidth (fwhm) $\sigma$ of the Lorentzian contribution of (*S*)-IBP/Me-*β*-CD inclusion complex (closed squares), (*R*,*S*)-IBP/Me-*β*-CD inclusion complex (open circles), and Me-*β*-CD (closed up triangles) at $T$ = 300 K. Error bars on $\sigma$ values are, on average, on the order of 7% for all the investigated samples.


dx.doi.org/10.1021/jp403099a | J. Phys. Chem. B 2013, 117, 11466−11472

inclusion complex and $\tau = 2.8 \pm 0.1$ ps for (*S*)-IBP/Me-*β*-CD and Me-*β*-CD systems.

Quite interestingly, the calculated elastic incoherent structure factor is in practice the same for both the complexes and the macrocycle, as shown in Figure 8. With the only purpose of

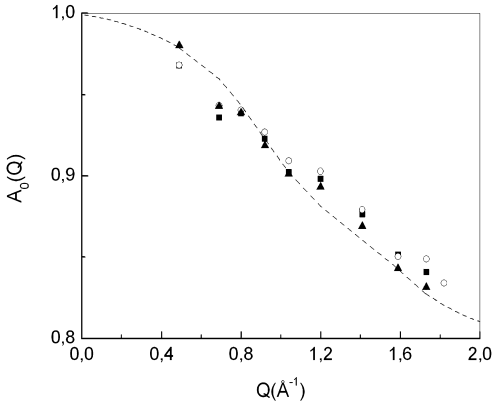


**Figure 8.** *Q*-dependence of $A_0(Q)$ for (*S*)-IBP/Me-*β*-CD inclusion complex (closed squares), (*R*,*S*)-IBP/Me-*β*-CD inclusion complex (open circles), and Me-*β*-CD (closed up triangles) at $T = 300$ K.

giving some quantitative detail on the dynamics of the different samples we applied an oversimplified model to describe the confined diffusive macromolecular dynamics. Therefore, consistent with the *Q*-independent behavior of the linewidths, we assumed that most of the diffusing hydrogen atoms belong to methyl groups in the Me-*β*-CD system that can perform random jump diffusion between three equidistant sites on a circle of radius $R = 1.1$ Å, and a fraction $f$ that move too slowly to be resolved in the experiment. In this context we can write

$$A_0(Q) = f + (1 - f)[1/3(1 + 2j_0(RQ))] \quad (4)$$

where $j_0(x)$ is first spherical Bessel function. The resulting fit, which is reported in Figure 8, provides the value of "immobile" hydrogen atoms of $f = 0.752 \pm 0.006$. This is consistent with an estimation of the number of hydrogen atoms belonging to methyl groups in Me-*β*-CD starting from chemical formula and considering the average degree of substitution.

These values suggest that the random-jump diffusing processes are mainly due to methyl groups and are quite similar in the complexes and in the macrocyle systems. This is in agreement with our previous FTIR-ATR measurements performed on the same systems that allowed us to hypothesize a similar complexation mechanism for both racemic and enantiomeric IBP, driven by the breaking-down of intermolecular hydrogen bonding of dimeric IBP, the release of enthalpy-rich water molecules from the hydrophobic cavity of CD, and their replacement with monomeric IBP molecules, with a consequent rearrangement of crystallization $H_2O$ in a new H-bond environment.[28] Again, as we mentioned above, the similar complexation of racemic and enantiomeric IBP is also confirmed by the aforementioned analysis of the vibrational density of states.

## CONCLUSIONS

In this paper, the chiral discrimination of ibuprofen (IBP) isomers by methyl-*β*-cyclodextrin (Me-*β*-CD), when forming inclusion "host–guest" complexes in solid state, has been probed by the investigation of their vibrational and relaxational internal dynamics, compared to that of the free "host" and "guest" molecules, through inelastic and quasi elastic neutron scattering.

The analysis of the vibrational density of states (VDOS), as obtained from INS analysis, gave evidence of a similar complexation mechanism for (*S*)-IBP and (*R*,*S*)-IBP, with a preferred inclusion mode that sees the isopropyl group of IBP restricted into the hydrophobic cavity of Me-*β*-CD.

The quasi-elastic term is well-reproduced by the superposition of a narrow *Q*-independent Lorentzian component and a flat background. This anharmonic internal dynamics revealed in the quasi elastic spectra of inclusion complexes and cyclodextrin is correlated with the rotational motions of $CH_3$ methyl groups of the systems. The analysis of the results confirmed, in agreement with INS data, a similar complexation mechanism for (*S*)-IBP and (*R*,*S*)-IBP.

## AUTHOR INFORMATION

### Corresponding Author

*Phone: +39-090-6765237; Fax: +39-090-395004; E-mail: majolino@unime.it.

### Notes

The authors declare no competing financial interest.

## ACKNOWLEDGMENTS

The author B. Rossi acknowledges the financial support of the Regione Veneto, being the beneficiary of a scholarship within the Programma Operativo Regionale FSE 2007-2013.

## REFERENCES

(1) Podlech, J. Origin of Organic Molecules and Biomolecular Homochirality. *Cell. Mol. Life Sci.* **2002**, *58*, 44–60.

(2) Jin, L. J.; Li, S. F. Y. Comparison of Chiral Recognition Capabilities of Cyclodextrins for the Separation of Basic Drugs in Capillary Zone Electrophoresis. *J. Chromatogr., B* **1998**, *708*, 257–266.

(3) Szejtli, J. *Comprehensive Supramolecular Chemistry (CDs)*; Szejtli, J., Osa, T., Eds.; Pergamon: Oxford, 1996.

(4) Takashima, Y.; Kawaguchi, Y.; Nakagawa, S.; Harada, A. Inclusion Complex Formation and Hydrolysis of Lactones by Cyclodextrins. *Chem. Lett.* **2003**, *32*, 1122–1123.

(5) Amajjahe, S.; Choi, S.; Muntenau, M.; Ritter, H. Pseudopolyanions Based on Poly(NIPAAM-co-*β*-Cyclodextrin Methacrylate) and Ionic Liquids. *Angew. Chem., Int. Ed.* **2008**, *47*, 3435–3437.

(6) Takashima, T.; Osaki, M.; Harada, A. Cyclodextrin-Initiated Polymerization of Cyclic Esters in Bulk: Formation of Polyester-Tethered Cyclodextrins. *J. Am. Chem. Soc.* **2004**, *126*, 13588–13589.

(7) Wenz, G.; Han, B.-H; Müller, A. Cyclodextrin Rotaxanes and Polyrotaxanes. *Chem. Rev.* **2006**, *106*, 782–817.

(8) Wenz, G. Recognition of Monomers and Polymers by Cyclodextrins. *Adv. Polym. Sci.* **2009**, *222*, 1–54.

(9) Alexander, J. M.; Clark, J. L.; Brett, T. J.; Stezowski, J. J. Chiral Discrimination in Cyclodextrin Complexes of Amino Acid Derivatives: Beta-Cyclodextrin/N-Acetyl-L-Phenylalanine and N-Acetyl-D-Phenylalanine Complexes. *Proc. Natl. Acad. Sci. U. S. A.* **2002**, *99*, 5115–5120.

(10) Núñez-Agüero, C. J.; Escobar-Llanos, C. M.; Díaz, D.; Jaime, C.; Garduño-Juárez, R. Chiral Discrimination of Ibuprofen Isomers in *β*-Cyclodextrin Inclusion Complexes: Experimental (NMR) and Theoretical (MD, MM/GBSA) Studies. *Tetrahedron* **2006**, *62*, 4162–4172.

(11) Tazerouti, F.; Badjah-Hadj-Ahmed, A. Y.; Meklati, B. Y.; Franco, P.; Minguillon, C. Enantiomeric Separation Of Drugs And Herbicides on a *β*-Cyclodextrin Bonded Stationary Phase. *Chirality* **2002**, *14*, 59–62.

(12) Salvatierra, D.; Sánchez-Ruiz, X.; Garduño-Juárez, R.; Cervelló, E.; Jaime, C.; Virgili, A.; Sánchez-Fernando, F. Enantiodifferentiation

by Complexation with β-Cyclodextrin: Experimental (NMR) and Theoretical (MD, FEP) Studies. *Tetrahedron* **2000**, *56*, 3035−3041.
(13) Kano, K.; Kamo, H.; Negi, S.; Kitae, T.; Takaoka, R.; Yamaguchi, M.; Okubo, H.; Hirama, M. Chiral Recognition of an Anionic Tetrahelicene by Native Cyclodextrins. Enantioselectivity Dominated by Location of a Hydrophilic Group of the Guest in a Cyclodextrin Cavity. *J. Chem. Soc., Perkin Trans.* **1999**, *2*, 15−22.
(14) Rekharsky, M. V.; Inoue, Y. Complexation Thermodynamics of Cyclodextrins. *Chem. Rev.* **1998**, *98*, 1875−1918.
(15) Piel, G.; Dive, G.; Evrard, B.; Van Hees, T.; de Hassonville, S. H.; Delattre, L. Molecular Modeling Study of β-CD Complexes with Miconazole. *Eur. J. Pharm. Sci.* **2001**, *13*, 271−279.
(16) Armstrong, D. W.; Yang, X. F.; Han, S. M.; Menges, R. A. Direct Liquid Chromatographic Separation of Racemates with an Alpha-Cyclodextrin Bonded Phase. *Anal. Chem.* **1987**, *59*, 2594−2596.
(17) Bikádi, Z.; Iványi, R.; Szente, L.; Ilisz, I.; Hazai, E. Cyclodextrin Complexes: Chiral Recognition and Complexation Behaviour. *Curr. Drug Discovery Technol.* **2007**, *4*, 282−294.
(18) Barbato, F.; La-Rotonda, M.; Quaglia, F. Interactions of Nonsteroidal Antiinflammatory Drugs with Phospholipids: Comparison Between Octanol/Buffer Partition Coefficients and Chromatographic Indexes on Immobilized Artificial Membranes. *J. Pharm. Sci.* **1997**, *86*, 225−229.
(19) Su, X. Y.; Al-Kassas, R.; Li Wan, Po, A. Statistical Modelling of Ibuprofen Release From Spherical Lipophilic Matrices. *Eur. J. Pharm. Biopharm.* **1994**, *40*, 73−76.
(20) Adams, S. S.; Bresloff, P.; Manson, C. Pharmacological Differences Between the Optical Isomers of Ibuprofen: Evidence for Metabolic Inversion Of The (-)-Isomer. *J. Pharm. Pharmacol.* **1976**, *28*, 256−257.
(21) Li, Z.; Zell, M.; Munson, E.; Grant, D. Characterization of Racemic Species of Chiral Drugs Using Thermal Analysis, Thermodynamic Calculation, and Structural Studies. *J. Pharm. Sci.* **1999**, *88*, 337−346.
(22) Pelrovich, G.; Kurkov, S.; Hansen, L.; Bauer-Brand, A. Thermodynamics of Sublimation, Crystal Lattice Energies, and Crystal Structures of Racemates and Enantiomers: (+)- and (±)-Ibuprofen. *J. Pharm. Sci.* **2004**, *93*, 654−666.
(23) Bogdanova, S.; Pareva, I.; Nikolova, P.; Tskavoska, I.; Muller, B. Interactions of Poly(Vinylpyrrolidone) with Ibuprofen and Naproxen: Experimental and Modeling Studies. *Pharm. Res.* **2005**, *22*, 806−815.
(24) Freer, A.; Bunyan, J.; Shankland, N.; Sheen, D. Structure of (S)-(+)-Ibuprofen. *Acta Crystallogr., Sect. C* **1993**, *49*, 1378−1380.
(25) Manzoori, J. L.; Amjadi, M. Spectrofluorimetric Study of Host/Guest Complexation of Ibuprofen with β-Cyclodextrin and its Analytical Application. *Spectrochim. Acta, Part A* **2003**, *59*, 909−916.
(26) Nerurkar, J.; Beach, J.; Park, M.; Jun, H. Solubility of (±)-Ibuprofen and S(+)-Ibuprofen in the Presence of Cosolvents and Cyclodextrins. *Pharm. Dev. Technol.* **2005**, *10*, 413−421.
(27) Crupi, V.; Majolino, D.; Venuti, V.; Guella, G.; Mancini, I.; Rossi, B.; Verrocchio, P.; Viliani, G.; Stancanelli, R. Temperature Effect on the Vibrational Dynamics of Cyclodextrin Inclusion Complexes: Investigation by FTIR-ATR Spectroscopy and Numerical Simulation. *J. Phys. Chem. A* **2010**, *114*, 6811−6817.
(28) Crupi, V.; Guella, G.; Majolino, D.; Mancini, I.; Paciaroni, A.; Rossi, B.; Venuti, V.; Verrocchio, P.; Viliani, G. Effect of the Chiral Discrimination on the Vibrational Properties of (R)-, (S)- and (R, S)-Ibuprofen/methyl-β-cyclodextrin Inclusion Complexes. *Philos. Mag.* **2011**, *91*, 1776−1785.
(29) Rossi, B.; Verrocchio, P.; Viliani, G.; Mancini, I.; Guella, G.; Rigo, E.; Scarduelli, G.; Mariotto, G. Vibrational Properties of Ibuprofen−Cyclodextrin Inclusion Complexes Investigated by Raman Scattering and Numerical Simulation. *J. Raman Spectrosc.* **2009**, *40*, 453−458.
(30) F.V. Sears, F. V. Slow Neutron Multiple Scattering. *Adv. Phys.* **1975**, *24*, 1−45.
(31) Lefort, R.; Morineau, D.; Guégan, R.; Ecolivet, C.; Guendouz, M.; Zanotti, J. M.; Frick, B. Incoherent Quasielastic Neutron Scattering Study of Molecular Dynamics of 4-n-octyl-4′-cyanobiphenyl. *Phys. Chem. Chem. Phys.* **2008**, *10*, 2993−2999.
(32) Bée, M. *Quasielastic Neutron Scattering: Principles and Applications in Solid-State Chemistry, Biology and Material Science*; Adam Hilger: Bristol and Philadelphia, 1988.
(33) Smith, J. C. Q. Protein Dynamics: Comparison of Simulations with Inelastic Neutron Scattering Experiments. *Rev. Biophys.* **1991**, *24*, 227−291.
(34) Wood, K.; Frölich, A.; Paciaroni, A.; Moulin, M.; Härtlein, M.; Zaccai, G.; Tobias, D. J.; Weik, M. Coincidence of Dynamical Transitions in a Soluble Protein and Its Hydration Water: Direct Measurements by Neutron Scattering and MD Simulations. *J. Am. Chem. Soc.* **2008**, *130*, 4586−4587.
(35) Plazanet, M.; Dean, M.; Merlini, M.; Huller, A.; Emerich, H.; Meneghini, C.; Johnson, M. R.; Trommsdorff, H. P. Crystallization on Heating and Complex Phase Behavior of α-cyclodextrin Solutions. *J. Chem. Phys.* **2006**, *125*, 154504−1,6.
(36) Sonvico, F.; Di Bari, M. T.; Bove, L.; Deriu, A.; Cavatorta, F.; Albanese, G. Mean Square Hydrogen Fluctuations in Chitosan/Lecithin Nanoparticles from Elastic Neutron Scattering Experiments. *Physica B* **2006**, *385−386*, 725−727.
(37) Fitter, J.; Lechner, R. E.; Dencher, N. A. Picosecond Molecular Motions in Bacteriorhodopsin from Neutron Scattering. *Biophys. J.* **1997**, *73*, 2126−2137.
(38) Springer, T. Quasielastic Neutron Scattering for the Investigation of Diffusive Motions in Solids and Liquids in *Springer Tracts in Modern Physics*; Springer: Berlin, 1972.
(39) Lovesey, S. W. *Theory of Neutron Scattering from Condensed Matter*; Adair, R. K., Elliott, R. J., Krumhansl, J. A., Marshall, W., Wilkinson, D. H., Eds.; Clarendon Press: Ottawa, Ontario, 1986.
(40) Taraskin, S. N.; Elliott, S. R. Connection Between the True Vibrational Density of States and That Derived From Inelastic Neutron Scattering. *Phys. Rev. B* **1997**, *55*, 117−123.
(41) Frick, B.; Richter, D. The Microscopic Basis of the Glass Transition in Polymers from Neutron Scattering Studies. *Science* **1995**, *267*, 1939−1945.
(42) Hédoux, A.; Guinet, Y.; Derollez, P.; Dudognon, E.; Correia, N. T. Raman Spectroscopy of Racemic Ibuprofen: Evidence of Molecular Disorder in Phase II. *Int. J. Pharm.* **2011**, *421*, 45−52.
(43) Crupi, V.; Majolino, D.; Paciaroni, A.; Stancanelli, R.; Venuti, V. Temperature-Dependent Dynamics of Water Confined in Nafion Membranes. *J. Phys. Chem. B* **2009**, *113*, 11032−11038.
(44) Hladoń, T.; Pawlaczyk, J.; Szafran, B. Stability of Ibuprofen in its Inclusion Complex with β-cyclodextrin. *J. Incl. Phen. Macrocycl. Chem.* **2000**, *36*, 1−8.
(45) Tozuka, Y.; Fujito, T.; Moribe, K.; Yamamoto, K. Ibuprofen-Cyclodextrin Inclusion Complex Formation using Supercritical Carbon Dioxide. *J. Inclusion Phenom. Macrocyclic Chem.* **2006**, *56*, 33−37.
(46) Hussein, K.; Türk, M.; Wahl, M. A. Comparative Evaluation of Ibuprofen/β-cyclodextrin Complexes Obtained by Supercritical Carbon Dioxide and Other Conventional Methods. *Pharm. Res.* **2007**, *24*, 585−592.
(47) Tayade, P. T.; Vavia, P. R. Inclusion Complexes of Ketoprofen with β-cyclodextrins: Oral Pharmacokinetics of Ketoprofen in Human. *Indian J. Pharm. Sci.* **2006**, *68*, 164−170.
(48) Farcas, A.; Jarroux, N.; Farcas, A. M.; Harabagiu, V.; Guegan, P. Synthesis and Characterization of Furosemide Complex in β-cyclodextrin. *Dig. J. Nanomater. Biostruct.* **2006**, *1*, 55−60.
(49) Nicolescu, C.; Aramă, C.; Monciu, C. M. Preparation and Characterization of Inclusion Complexes between Repaglinide and β-cyclodextrin, 2hydroxypropylβ- cyclodextrin and Randomly Methylated β-cyclodextrin. *Farmacia* **2010**, *58*, 78−88.
(50) Frick, B.; Fetters, L. J. Methyl Group Dynamics in Glassy Polysoprene: a Neutron Backscattering Investigation. *Macromolecules* **1994**, *27*, 974−980.